

The passage involves an increase in the intensity of the scattered polariton signal by many orders of magnitude and is illustrated in Fig. 5. In numerical simulations, the pumping amplitude $\mathcal{E}(t)$ was first switched on at 99% of its maximum for about 100 ps, then increased slowly to the maximum value for ~ 1000 ps, and then switched off within another 100 ps.

The physical mechanism of the above passage is due to the fact that the decay of a pumping polariton to the S and I polaritons becomes parametrically unstable when a certain critical pumping intensity is reached, and due to the presence of an absolutely unstable negative slope region on the S-like plot showing the way the exciton polarization $\mathcal{P}(k_p, t)$ at the pumping angle varies with pumping amplitude. The parametric decay instability is similar to that in Ref. [12] discussing the Mandelstam – Brillouin scattering of an intense polariton wave. It is only this type of instability which was considered in the previous analyses [6, 8–10] of the parametric scattering of MC polaritons. Our calculations show, however, that due to the development of parametric scattering instability, the response of a nonlinear oscillator at the pumping angle may become unstable during the actual evolution of a system. As a result, instead of the parametric build-up of macrofilled modes for $k_s \neq 0$ and $k_i \neq 2k_p$, the spectrum of the scattered polariton signal is strongly rearranged, acquiring maxima at $k_s \approx 0$ and $k_i \approx 2k_p$, and an increase by several orders of magnitude in the total scattered intensity is observed. This behavior is qualitatively consistent with that observed in experiment.

Acknowledgments. The authors are grateful to L V Keldysh for numerous discussions, and M Skolnik for providing the samples. Partial financial support from the RFBR and INTAS is gratefully acknowledged.

References

1. Weisbuch C et al. *Phys. Rev. Lett.* **69** 3314 (1992)
2. Baumberg J J et al. *Phys. Rev. B* **62** R16247 (2000)
3. Kulakovskii V D et al. *Usp. Fiz. Nauk* **170** 912 (2001) [*Phys. Usp.* **43** 853 (2001)]
4. Stevenson R M et al. *Phys. Rev. Lett.* **85** 3680 (2000)
5. Tartakovskii A I, Krizhanovskii D N, Kulakovskii V D *Phys. Rev. B* **62** R13298 (2000)
6. Savvidis P G et al. *Phys. Rev. Lett.* **84** 1547 (2000)
7. Ciuti C et al. *Phys. Rev. B* **62** R4825 (2000)
8. Ciuti C, Schwendimann P, Quattropani A *Phys. Rev. B* **63** 041303(R) (2001)
9. Savvidis P G et al. *Phys. Rev. B* **64** 075311 (2001)
10. Saba M et al. *Nature* **414** 731 (2001)
11. Gippius N et al., in *Proc. of the 26th Intern. Conf. on the Physics of Semiconductors, 29 July–2 Aug. 2002, Edinburgh, UK* (London: IOP, 2002) p. G4-6
12. Keldysh L V, Tikhodeev S G *Zh. Eksp. Teor. Fiz.* **90** 1852 (1986) [*Sov. Phys. JETP* **63** 1086 (1986)]

PACS numbers: 71.35.Ee, 71.35.Ji

DOI: 10.1070/PU2003v046n09ABEH001644

Magnetically stabilized multiparticle bound states in semiconductors

N N Sibel'din

1. Introduction

Under laboratory conditions, a magnetic field acting on an atom removes the degeneracy with respect to the directions of the angular momentum (Zeeman and Paschen – Back effects)

and causes a slight diamagnetic shift of the high-lying energy levels; however, the inner structure of the atom (electron density distribution) and its energy spectrum (neglecting the splitting of the levels in a magnetic field, which is small compared to the atomic electron binding energy) remain virtually unchanged. The effect of a magnetic field becomes significant when the field strength is sufficiently large, such that the cyclotron energy of a free electron, $\hbar\omega_c = \hbar eH/cm$, where m is the electron mass, becomes comparable to the electron binding energy in the atom, and the magnetic length $a_H = \sqrt{\hbar/eH}$ is of the order of the atomic radius. In the case of the hydrogen atom, for example, this implies the field strength $H \sim 10^9$ Oe, which is beyond the reach of modern experiments. We therefore depend on astrophysical observations or experiments on model systems when wish to draw information on the properties of atoms in strong magnetic fields.

The most attractive objects for such studies are apparently excitons and the atoms of hydrogen-like impurities in semiconductors. The ground-state energy and the Bohr radius of an exciton (an atom of a hydrogen-like impurity) in a semiconductor crystal are given by the Bohr formulas, which in this case take the form

$$E_{\text{ex}} = -\frac{m^* e^4}{2\kappa^2 \hbar^2}, \quad (1)$$

$$a_{\text{ex}} = \frac{\kappa \hbar^2}{m^* e^2}, \quad (2)$$

where κ is the dielectric constant of the crystal, and m^* is the reduced effective mass of an electron and a hole (the effective mass of an electron or a hole for shallow donors and acceptors, respectively). Due to the large dielectric constant of the medium and because of the small effective masses of the electrons and holes, the binding energies of excitons, $|E_{\text{ex}}|$, and of hydrogen-like impurities are typically 3 to 4 orders of magnitude smaller than for the hydrogen atom, and their Bohr radii 2 to 3 orders of magnitude larger. In the fields of equal strength, the cyclotron frequency of charge carriers in a semiconductor is m/m^* times that of a free electron, making even $H \sim 10^3 - 10^4$ Oe a strong field for excitons and the atoms of shallow impurities.

The behavior of hydrogen-like impurities in strong magnetic fields was treated theoretically in Refs [1–3], and the behavior of excitons in Refs [4–6]. A magnetic field stabilizes excitonic (atomic) states. In weak fields, the binding energy increases because the free-electron energy (the cyclotron frequency) increases linearly with the field strength, whereas that of a bound electron in an atom increases quadratically (diamagnetic shift). In ultrahigh fields ($\hbar\omega_c \gg |E_{\text{ex}}|$), the centripetal force acting on an electron orbiting the nucleus in the plane perpendicular to the magnetic field direction is dominated by the Lorentz force (the Coulomb interaction of the electron with the nucleus — or with a hole in an exciton — can be treated as a perturbation). An exciton (atom) is strongly anisotropic; its shape is an ellipsoid of revolution oriented along the magnetic field, with semi-axes a_{ex} and a_H in the longitudinal and transverse directions, respectively. The exciton binding energy $|E_{\text{ex}}|$ increases in proportion to $\ln^2 H$ as the field strength is increased [6]. Such excitons were called diamagnetic [7].

Experimentally, effects related to the increase in the ionization energy of shallow donors in a magnetic field were first observed in heavily doped indium antimonide (magnetic

freezing-out of impurities [8]). A wealth of information about the properties of excitonic states was obtained in magneto-optical experiments which are discussed in great detail in a review [7] and a monograph [9].

Apart from atomic bound states, more complicated types of bound states (for example, molecular) can also be stabilized by a magnetic field. Thus, an increase in the magnetic field strength leads to an increase in the exciton effective mass in the direction transverse to the magnetic field [6], which allows localization of excitons near defects and impurity atoms which are unable to bind an exciton in the absence of a field [10]. The effect of a strong magnetic field on the properties of bound excitons was discussed theoretically in Refs [10, 11]. Similar to excitons that are bound in the absence of a magnetic field [12, 13], whose emission lines generally dominate the luminescence spectra even of sufficiently pure semiconductors at low temperatures and moderate excitation levels [14], magnetic-field-stabilized exciton-impurity complexes (EICs) (bound excitons) possess giant oscillator strengths [10]. Magnetically stabilized EICs were discovered experimentally in indium antimonide in our studies [15, 16].

Generally, molecular states can be both stabilized and destabilized by a magnetic field. When the lower energy level of an unbound triplet state of an exciton molecule (biexciton) shifts below the singlet level as a result of spin splitting in a strong field, the molecule becomes unstable and the bi-exciton luminescence line disappears [17]. In ultrahigh magnetic fields, however, stable spin-aligned (triplet) biexcitons [18] (or hydrogen molecules [19]) can form.

Perhaps of particular interest is the behavior of condensed matter in ultrahigh magnetic fields. A good model system for experimental studying phenomena of this kind is the condensed phase of excitons in semiconductors, called the electron–hole liquid (EHL) [20–24]. It has been shown theoretically that under certain conditions an ultrahigh magnetic field should produce a ‘highly compressed’ EHL whose density greatly exceeds the inverse volume of a diamagnetic exciton and whose energy per particle pair is much greater in absolute value than the exciton binding energy [25, 26]. It has also been shown that the dominant contribution to the energy of attraction in the liquid comes from the spatial correlation of the particles located at neighboring Landau cylinders. The strong compression condition for the electron–hole plasma is expressed by the first half of the inequality [25]

$$(a_{\text{ex}} a_H^2)^{-1} \ll n \ll a_H^{-3}. \quad (3)$$

In the strong compression region, an electron–hole system constitutes a degenerate Fermi liquid, and its energy, as a

function of the density n , has a minimum at $n = n_0$. In the ultraquantum limit, i.e., when the right half of inequality (3) is satisfied, the equilibrium density of a strongly compressed electron–hole liquid is $n_0 \propto H^{8/7}$, and the energy per particle pair in the ground state of the liquid is $|E(n = n_0)| \equiv |E_0| \propto H^{2/7}$. Because the ionization energy of diamagnetic excitons builds up more slowly with increasing field strength, the stability of the liquid state — which is characterized by the work function $\varphi = E_{\text{ex}} - E_0$ of excitons in a liquid — should increase in a strong magnetic field as the field intensity grows. Furthermore, in a strong magnetic field the liquid phase may prove to be stable ($\varphi > 0$) even if in the absence of the field it is not. Electron–hole liquid stabilized by a magnetic field $H > 20$ kOe was discovered by us in indium antimonide [15].

What follows are the results of the experimental study of magnetic-field-stabilized EICs and EHL in indium antimonide. Indium antimonide (InSb) is the most suitable material to study the effects of a strong magnetic field on weakly bound electronic states. The electron effective mass in this semiconductor is extremely small ($m_e \cong 0.014m$), so that even for a field strength of a few kilooersted the magnetic length is $a_H < a_{\text{ex}}$, and the electron cyclotron energy exceeds the exciton Rydberg. On the other hand, with current technology of growing this compound, perfect single crystals with low content of residual impurities can be prepared. More detailed information and a bibliography on the experiments described below can be found in Ref. [27] (EICs) and Refs [28, 29] (EHL).

2. Magnetically stabilized exciton-impurity complexes

The experiments were performed on pure n-type crystals of indium antimonide at temperatures T between 2 K and 4.2 K. The parameters of the samples (the difference between the concentration of donors N_D and that of acceptors N_A , and the degree of compensation $k = N_A/N_D$) are listed in Table 1. The photoluminescence spectra of the samples were studied at sufficiently low quasi-CW excitation levels using radiation of a continuous He–Ne laser with a wavelength of 3.39 μm and a peak power of about 15 mW. The light spot on the surface of the sample was ~ 0.3 mm in diameter.

In the absence of a magnetic field, the principal line of edge luminescence (lower spectrum in Fig. 1a) for sufficiently pure n-InSb lies almost entirely at energies smaller than the crystal bandgap E_g (the currently accepted value is $E_g = 236.8 \pm 0.2$ meV at $T = 2$ K [30]). The line is due to electron transitions from shallow donor levels to the valence band, and its shape and spectral position are determined by the large-scale fluctuations of the impurity potential [31] (other views on the nature of luminescence spectra are

Table 1. Parameters of n-InSb samples and the approximate values of magnetic field strengths corresponding to the emergence of EIC luminescence lines.

Sample number	$N_D - N_A$, 10^{14} cm^{-3}	k	$I_{A_{1,2}}/I_0$	$I_{A_3}/I_{A_{1,2}}$	H_r , kOe		
					EIC _I	EIC _{II}	EIC _{III}
1	0.3	0.8	0.04	0.3	37	7–9	7–9
2	0.7	0.7	0.03	0.8	18	—	9
3	0.96	0.6	0.01	5	—	—	14
4	1.0–2.0	0.5	0.01–0.02	0.5	—	5–7	—
5	0.6	0.6	—	—	—	—	—

Note. A dash indicates that the corresponding line is absent in the emission spectrum.

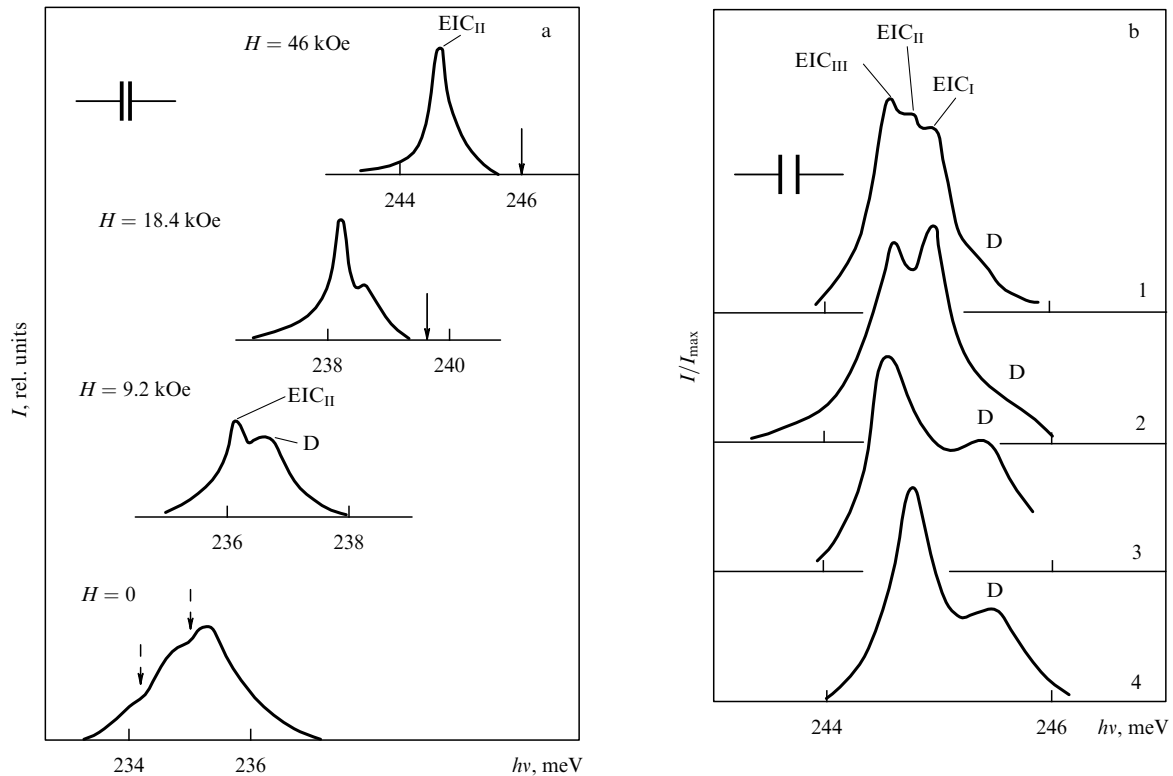


Figure 1. Luminescence spectra of (a) sample No. 4 for various magnetic field strengths, and (b) samples Nos 1–4 (spectra are labelled by sample numbers) in a field of strength $H = 46$ kOe. Excitation intensity was 10 W cm^{-2} , $T = 2 \text{ K}$. D is the donor emission line; EIC_I, EIC_{II}, and EIC_{III} are the lines of the exciton-impurity complexes. In (a) solid arrows indicate the position of the energy level of a free diamagnetic exciton as determined from magnetoreflection spectra, and broken arrows ($H = 0$) locate the absorption lines of atmospheric water vapors. In (b), the intensity of each spectrum at a maximum is $I_{\text{max}} = 1$.

discussed in Refs [27, 31, 32], where the literature on the subject can also be found). Because the electron effective mass in indium antimonide is small, the exciton binding energy is also very small ($|E_{\text{ex}}| \approx 0.5 \text{ meV}$ [30]), as is the dissociation energy of EICs on shallow donors and acceptors with $E_i < 0.5 \text{ meV}$. Therefore, free- and bound-exciton lines are not usually observed in emission spectra in the absence of a magnetic field.

In addition to the principal luminescence line, in the energy range $E_g - E_A \lesssim hv < E_g$, where E_A is the ionization energy of shallow acceptors, weak lines of recombination radiation were also observed, with peak positions at 226.7–228.0 meV and 223.5–224.0 meV. The higher-frequency line is apparently a superposition of at least two components. Most likely this line corresponds to the zinc and cadmium acceptors, which usually are present in pure indium antimonide and have nearly the same ionization energies. The lower-frequency line is due to transitions to the levels of an unknown acceptor impurity. Table 1 lists the average intensities at the peaks of the high- and low-frequency acceptor lines. The intensity of the high-frequency line $I_{A_{1,2}}$ (the subscript $A_{1,2}$ emphasizes that this line consists of several components) is given in relation to that of the principal emission line I_0 , and the intensity of the low-frequency line I_{A_3} in relation to $I_{A_{1,2}}$. It should be noted that the intensity of an acceptor emission line reflects the content of acceptor atoms of a certain chemical nature in the sample, whereas the degree of compensation as obtained from electrical measurements is related to the total concentration of acceptors (including deep ones) in the crystal.

In terms of the magnetic field behavior of emission spectrum, the simplest sample is No. 5, in which the concentration of acceptors and the total concentration of donors and acceptors are the lowest among all the samples studied, and in which, most importantly, there are no acceptor lines in the luminescence spectrum (see Table 1). Over the entire magnetic field range studied ($H = 0$ –56 kOe), the emission spectrum of this sample exhibits a single line, whose half-width at first decreases with increasing field, reaches a value of $\approx 0.5 \text{ meV}$ at $H \approx 20 \text{ kOe}$, and then remains unchanged. As the field strength is increased, the emission line shifts to higher energies (in weak fields this shift is nonlinear in field strength), and its intensity decreases somewhat. This line is shifted to lower frequencies considerably with respect to the long-wavelength component of the spectrum of exciton magnetoreflection, whose characteristics were measured to determine the ground-state energy position of a free diamagnetic exciton. As is the case with the absence of a magnetic field, the observed emission line is due to the electron transitions from shallow donor levels to the valence band.

The principal luminescence lines of other samples behave in a similar way when increasing the magnetic field. They shift to higher frequencies, get narrower, and decrease in intensity. At the same time, the luminescence spectra of samples Nos 1–4 exhibit emission lines of exciton-impurity complexes in a magnetic field. For example, in the emission spectrum of sample No. 4, an EIC line appears on the long-wavelength wing of the principal emission band in a field of strength $H_r = 5$ –7 kOe. Its intensity heightens as the field strength is

increased, and it dominates the spectrum in strong fields (Fig. 1a, EIC_{II} line). In a strong magnetic field, the half-width of the emission line is 0.2–0.4 meV. In a weak field, the short-wavelength shift of the peak of the EIC emission line depends nonlinearly on the field strength, whereas in a sufficiently strong field a linear dependence is observed. In a strong magnetic field, the energy spacing between the peak of the EIC emission line and the position of the long-wavelength component of the exciton magnetoreflection spectrum (i.e., the optical dissociation energy of exciton-impurity complexes) increases weakly with magnetic field strength and reaches $E_i^{\text{op}} \cong 1.2$ meV for $H = 23$ kOe, and $E_i^{\text{op}} \cong 1.4$ meV for $H = 46$ kOe.

In the remaining samples (Nos 1–3), one to three magnetic-field-stabilized EIC emission lines are observed. Qualitatively, their behavior with the variation of the magnetic field is the same as for the EIC_{II} emission line in sample No. 4, except that the lines arise at different field strengths. In sample No. 3, only the longest-wavelength EIC emission line is observed (EIC_{III} line), which appears at $H_r \sim 14$ kOe. In the spectrum of sample No. 2, two EIC emission lines appear successively as the magnetic field strength is increased: the longest-wavelength (EIC_{III}) at $H_r \sim 9$ kOe, and the shortest-wavelength (EIC_I) at $H_r \sim 18$ kOe. The luminescence spectrum of sample No. 1 is particularly rich in spectral lines. In it, all three of the discovered emission lines of exciton-impurity complexes — namely, EIC_{III}, EIC_{II}, and EIC_I lines — are observed. These lines appeared in the luminescence spectrum successively, starting from $H_r = 7–9$ kOe. It is hard to say, however, which of the two long-wavelength lines, EIC_{III} or EIC_{II}, emerges at a lower field strength. On the other hand, in a magnetic field of strength $H = 14$ kOe these lines were reliably resolved; the spacing between their peaks was $\cong 0.2$ meV and remained unchanged with further increase in field strength. The EIC_I emission line appeared at $H_r \cong 37$ kOe. In a field of strength $H = 46$ kOe, all three emission lines are clearly seen; the spacing between the peaks of neighboring lines was $\cong 0.2$ meV, and it was field-independent for $H > 46$ kOe. The luminescence spectra of samples Nos 1–4 in a field of strength $H = 46$ kOe are shown in Fig. 1b. Table 1 lists the values of the magnetic field strength H_r at which the emission lines of the corresponding EICs appeared in various samples.

The observed EICs constitute a diamagnetic exciton bound on a neutral shallow acceptor. The analysis of the experimental data summarized above, combined with a correlation between the emission line intensities of acceptors and the presence (or lacking) of EIC emission lines in the spectra of various samples (see Table 1), supports and details this conclusion. In sample No. 5, for example, neither acceptor nor EIC emission lines are seen. Sample No. 3 is characterized by a relatively weak acceptor emission intensity $A_{1,2}$ and shows the strongest A_3 emission due to the recombination of electrons with holes residing on acceptors with lower-lying energy levels. Therefore, the single EIC_{III} line observed on this sample can be ascribed to excitons that are bound on the acceptors responsible for the A_3 emission. In the same vein, it can be concluded that the emission lines EIC_I and EIC_{II} are due to excitons localized on the acceptor atoms of various chemical elements to which the composite emission line $A_{1,2}$ corresponds (see the discussion at the beginning of this section). Ascribing the emission lines EIC_I, EIC_{II}, and EIC_{III} of the exciton-impurity complexes to the acceptor

emission lines $A_{1,2}$ and A_3 , respectively, is generally consistent with the body of data summarized in the table.

Further arguments in favor of this picture are the facts (1) that the dissociation energy of exciton-impurity complexes increases from EIC_I to EIC_{III}, i.e., for excitons bound on the deeper acceptors, and (2) that the strength of a magnetic field needed to stabilize the corresponding EIC increases as the dissociation energy of the complex decreases. As seen from Table 1, samples No. 1 and No. 2 make this latter fact especially clear. On the other hand, it can hardly be expected that the emission line of excitons bound on acceptor atoms of a certain chemical nature will turn up in the luminescence spectra of different samples at exactly the same field strength. The reason is that the emission lines of complexes appear against the background of the principal luminescence band, whose intensity is quite large and varies from sample to sample, whereas the intensity of a particular emission line of bound excitons depends on the concentration of the corresponding acceptors, which is different in various samples. The superposition of neighboring emission lines of exciton-impurity complexes is another complicating factor in determining the value of the magnetic field corresponding to the appearance of a new line.

To summarize the above discussion, binding of excitons at shallow acceptors of different chemical nature in indium antimonide can lead to the formation of magnetic-field-stabilized exciton-impurity complexes. The luminescence spectra of these complexes exhibit characteristic narrow lines, whose intensity significantly (by a factor of tens in our samples) exceeds that of the corresponding acceptor emission lines. It should be emphasized that EICs were observed in our experiments in the n-InSb samples of maximum purity, and even though these samples differ only slightly from one another in the concentrations of the major and compensating impurities as determined from electric measurements, their luminescence spectra in a magnetic field differ considerably in the number and intensity of EIC emission lines. Thus, magnetic-field-stabilized EIC emission lines can serve as very sensitive indicators for determining the content and chemical nature of shallow acceptors in indium antimonide.

We now proceed to discuss how excitation intensity and temperature affect the intensity of EIC emission. The way the luminescence intensity of the complexes depends on the excitation level was examined in detail in samples No. 4 at $T = 2$ K. At relatively low pumping levels, the EIC luminescence intensity increases linearly with excitation power. At high excitation levels (in excess of ≈ 50 W cm⁻²), this dependence considerably weakens and tends to saturate.

The dependence of the spectra of recombination radiation on temperature was studied at low excitation intensity of about 10 W cm⁻² in samples No. 4, whose donor emission line has a marked intensity in a strong magnetic field at $T = 2$ K. On increasing the temperature from $T = 2$ K, the intensity of the EIC emission line decreased gradually, whereas that of the donor line increased somewhat, and its peak shifted towards longer wavelengths. At temperatures close to $T = 4.2$ K, a donor emission line dominated the luminescence spectrum. The temperature dependence of the EIC_{II} emission intensity is satisfactorily described by the expression

$$I_i = \frac{I_0}{1 + CT^{3/2} \exp(-E_i/kT)}, \quad (4)$$

where I_0 is the luminescence intensity of complexes at $T = 0$, E_i is the EIC dissociation energy, and the coefficient

$$C = \frac{g_A g_{ex}}{g_i} \left(\frac{M_d k}{2\pi\hbar^2} \right)^{3/2} \frac{\sigma v_T \tau_i}{1 + \sigma v_T \tau_{ex} N_A}, \quad (5)$$

where g_A , g_{ex} , and g_i are the corresponding degeneracy factors, M_d is the density-of-states effective mass of excitons, which is a combination of the longitudinal and transverse masses in a magnetic field, τ_i and τ_{ex} are the lifetimes of bound and free excitons, respectively, σ is the cross section for binding an exciton at a center, and v_T is the exciton thermal velocity. By processing data on the temperature dependence of EIC emission line intensity, the adjustable parameters E_i and C in formula (4) were determined. In a field of strength $H = 9.2$ kOe, the adjustable parameter E_i — i.e., the thermal dissociation energy E_i^T of the complexes — equals $\cong 1.1$ meV and is likely to be close to the optical dissociation energy. As the field strength increases to $H = 23$ kOe, this parameter decreases to $E_i^T \cong 0.6$ meV and then remains unchanged with further increase in the field strength, whereas the dissociation energy of the complexes as obtained from optical measurements (i.e., the optical dissociation energy) increases from $E_i^{op} \cong 1.2$ meV at $H = 23$ kOe to $E_i^{op} \cong 1.4$ meV at $H = 46$ kOe.

Thus we see that in a sufficiently strong magnetic field the thermal dissociation energy of the complexes is much lower than the optical. On the other hand, the obtained values of E_i^T approximately correspond to the energy spacing between the peak of the EIC_{II} emission line and that of the donor line. We can assume therefore that the electrons released by the thermal dissociation of an EIC move to shallow donor levels in the density-of-state tail of the conduction band. Other evidence of this fact is that the intensity of the donor emission line increases with increasing temperature. This process of dissociation of complexes is accompanied by a corresponding inverse process in which donor electrons are captured by acceptor A^+ ions.

Thus, the results obtained show that the magnetically stabilized exciton-impurity complexes observed in indium antimonide constitute an exciton bound on a neutral acceptor and that the formation of these complexes proceeds in two stages: first a neutral acceptor A^0 binds a hole and thus transforms to an A^+ center, and then this latter captures an electron from one of the donors located nearby.

3. Magnetically stabilized electron–hole liquid

It is well known that an electron–hole liquid (EHL) forms in a semiconductor at low temperatures and high excitation levels. In the experiments to be described in this section, the samples were excited by radiation of a cw YAG:Nd³⁺ laser with a wavelength of 1.06 μm and a peak power of 1 W, at $T = 1.8$ – 2 K. While the emission line of magnetically stabilized EHL was observed in all of the samples studied, detailed measurements were performed on samples No. 4: the EHL line in these samples was the strongest, and its luminescence spectrum is relatively simple (there is only one emission line from magnetically stabilized EICs). Therefore in what follows only the data taken from these samples are discussed.

Recombination radiation spectra of one of these samples, obtained at relatively low excitation levels in a magnetic field of strength $H = 46$ kOe, are depicted in Fig. 2a (spectrum 3) and in the inset to Fig. 2b. These spectra contain a more

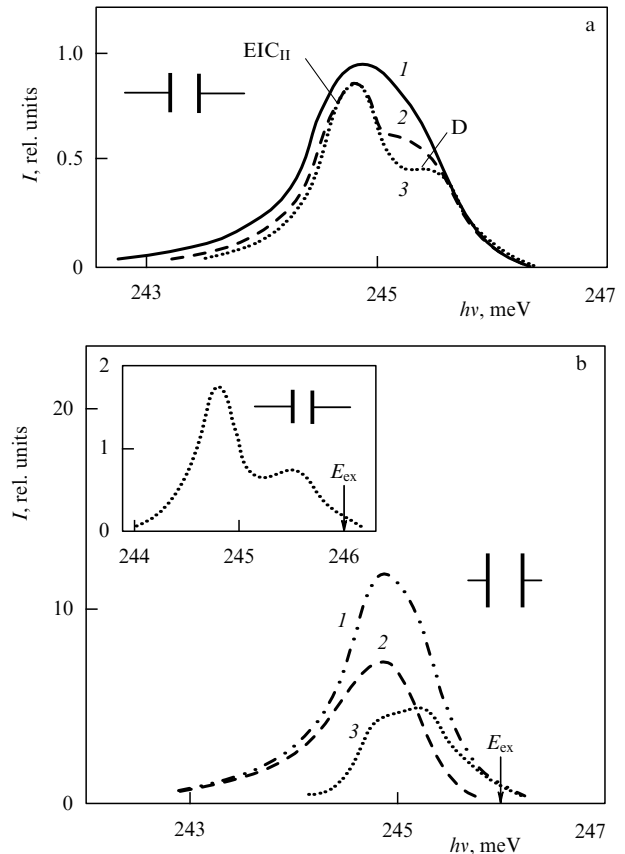


Figure 2. Luminescence spectra in a magnetic field of strength $H = 46$ kOe: (a) spectra for excitation intensity $P = 210$ W cm^{-2} (1), 140 W cm^{-2} (2), and 100 W cm^{-2} (3). Spectra are normalized so that emission intensities at $h\nu = 245.7$ meV are equal; (b) spectra for $P = 500$ W cm^{-2} . Modulation depth is 100% (1) and 20% (2). Spectrum 3 is obtained as the difference of spectra 1 and 2. The arrow indicates the energy of the transition to the lowest state of a diamagnetic exciton. The inset exemplifies the spectrum at low excitation level ($P \cong 50$ W cm^{-2}).

intense D line than does the spectrum shown in Fig. 1a, even though the respective samples have similar parameters and are cut from the same ingot. The luminescence spectra change their shape in a qualitatively different manner with increasing pumping intensity in a strong ($H > 20$ kOe) and in a relatively weak magnetic field. Emission spectra in a field of strength $H = 46$ kOe, observed at various pumping levels, are shown in Fig. 2a. As the pumping power increases, the intensity of the donor line increases at a higher rate than that of the EIC emission line. As a result, these emission lines merge into one relatively broad band. It is also seen from Fig. 2a that the emission spectrum broadens towards longer wavelengths and that it acquires a ‘tail’ extending towards lower energies. At the same time, the short-wavelength wing of the resulting spectrum has virtually the same shape as the donor line.

In a relatively weak field ($H < 20$ kOe), the emission spectrum exhibits quite different behavior. Here too, increasing pumping intensity leads to the disappearance of structures in the luminescence spectrum, but now it is the short-wavelength, rather than long-wavelength, wing of the structureless emission band which increases in extension. In what follows, only the results obtained in a strong magnetic field will be discussed.

Measurements of the excitation level dependences of luminescence intensity at various energies of recombination radiation quanta showed that at high pumping powers not only the luminescence of the EIC line, but also that of the donor line, starts to saturate in intensity. On the other hand, the emission intensity in the low-frequency tail of the spectrum increases practically linearly with the level of excitation. The low-frequency tail, whose luminescence intensity depends on the pumping power in a manner different from that for the two originally present spectral components, is due to the appearance (on the long-wavelength edge of the spectrum) of a new emission band which, because of the strong difference in these dependences, was separated out from the resulting spectrum using a technique that relies on the registration of the luminescence spectrum differential with respect to the excitation intensity.

The emission spectra obtained by high-power pumping at 100% (spectrum 1) and 20% (spectrum 2) excitation intensity modulation depths are displayed in Fig. 2b. The latter of these spectra is built from the experimental one in such a way that the intensity of the separated band corresponds to a modulation depth of 100%. Spectrum 3 in Fig. 2b was obtained as the difference of spectra 1 and 2. It is located in the same energy interval as the emission spectrum for lower excitation levels (inset to Fig. 2b). However, in accordance with the discussion above, the emission lines of donors and EICs are not resolved in the difference spectrum 3. In a weaker pumping regime, both lines are clearly seen in the difference spectrum.

By applying an electric field sufficient to cause the impact ionization of shallow donors and EICs, the luminescence lines of these formations can be made to quench, making it possible to separate from the emission spectrum a long-wavelength band that arises in the high-power pumping regime. The shape of the long-wavelength band separated in this way was close to that of the differential spectrum 2 (Fig. 2b) at excitation intensities in excess of 250 W cm^{-2} .

Thus, the above results show that in a magnetic field $H > 20 \text{ kOe}$, the long-wavelength edge of the indium antimonide luminescence spectrum exhibits an additional emission band at high pumping levels, which can be separated out from the resulting spectrum by using an emission spectrum detection technique differential with respect to excitation intensity or, alternatively, by applying an electric field. Unlike the other two components present in the spectrum, the intensity of this band increases as the electric voltage across the sample is increased. This means that the long-wavelength band is related to the recombination of the electrons and holes occupying states which are not depopulated in an electric field, even though in terms of its energy position the long-wavelength band is close to the emission lines of donors and EICs — the states which are destroyed by impact ionization. Therefore, the electronic states under study are significantly different in nature as compared with states of atomic and molecular types, i.e., states of systems involving a small number of interacting particles (impurity atoms, free and bound excitons, etc.).

It can be concluded from the behavior of the long-wavelength emission band in an electric field that the band is related to the particle recombination in the electron–hole plasma whose energy is reduced due to interparticle interactions. The fact that the intensity of the band grows in an electric field, whereas its low-frequency edge shape remains unchanged, suggests an increase in the volume that plasma

occupies in the sample. The violet edge of the long-wavelength band is shifted considerably to lower energies relative to the transition energy to the lowest state of a free exciton (Fig. 2b), i.e., the plasma particles have a smaller energy than electron–hole pairs bound into excitons. From this it can be concluded that we are dealing with a plasma of interacting particles, which is stable with respect to decay to free excitons — that is, with an electron–hole liquid. Because heating a plasma of free charge carriers in an electric field should broaden the short-wavelength wing of the plasma emission line, the fact that the shape of a long-wavelength band is independent of how the band is separated out from the total luminescence spectrum — i.e., whether by applying an electric field or by using 20% excitation intensity modulation — lends further support for the interpretation of this band as an EHL emission line.

It is known that one of the most compelling arguments for attributing some luminescence band to the EHL emission is a good correspondence of the shape of this band to the theoretical description. In addition, an analysis of the emission line shape makes it possible to reliably determine the characteristic energies of liquid particles and to find the liquid density [20–24].

The shape of the emission band of magnetically stabilized EHL in indium antimonide can be analyzed by using the usual expression for direct allowed transitions:

$$I(h\nu) \propto v^2 g(h\nu) f_e f_h, \quad (6)$$

where f_e and f_h are Fermi distribution functions for electrons and holes with Fermi energies E_{F_e} and E_{F_h} , respectively, and where the density of states is described by the formula

$$g(h\nu) = \frac{\sqrt{2m_r}}{(2\pi\hbar)^2} \frac{eH}{c} \times \sqrt{\frac{(h\nu - E_{gL})/\Gamma + \sqrt{[(h\nu - E_{gL})/\Gamma]^2 + 1}}{2\Gamma\{[(h\nu - E_{gL})/\Gamma]^2 + 1\}}}. \quad (7)$$

Here m_r is the reduced effective mass of the electrons and holes in the bands between which the recombination transitions occur, E_{gL} is the renormalized band gap in the EHL, and the parameter Γ characterizes the damping that removes the density-of-states singularities in the neighborhood of Landau levels.

Without detailing here the calculations and their underlying assumptions — the interested reader is referred to the original paper [29] — we outright present the results and then raise some points concerning them. The luminescence spectrum of an EHL in a magnetic field $H = 55.2 \text{ kOe}$, obtained using differential technique, and the results of calculations using formulas (6) and (7) are given in Fig. 3. By fitting the calculated spectrum to the experimental one, the damping parameter $\Gamma = 0.55 \text{ meV}$, renormalized band gap $E_{gL} = 246.26 \text{ meV}$, and the sum of the electron and the hole Fermi energies $E_F = 0.95 \text{ meV}$ were determined. With the knowledge of the Fermi energy, it was possible to find the density of the liquid: $n_0 = 6.7 \times 10^{15} \text{ cm}^{-3}$.

A similar procedure was used in processing differential luminescence spectra taken for other values of magnetic field strength (these values correspond to the experimental points in Fig. 4). The damping parameter Γ was independent of the magnetic field strength within experimental error, its average

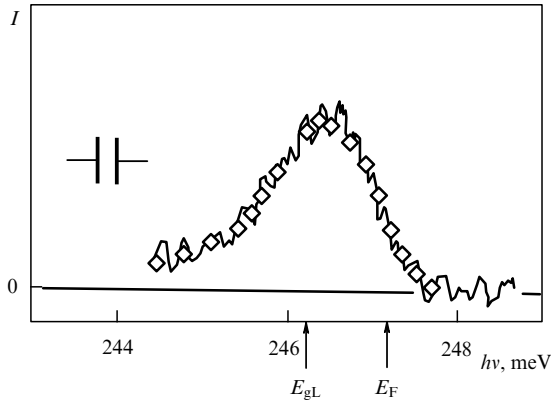


Figure 3. EHL luminescence spectra obtained experimentally (solid line) and calculated (rhombi) from Eqns (6) and (7). $H = 55.2$ kOe, and $P = 500$ W cm $^{-2}$. Arrows indicate E_{gL} and E_F obtained by fitting.

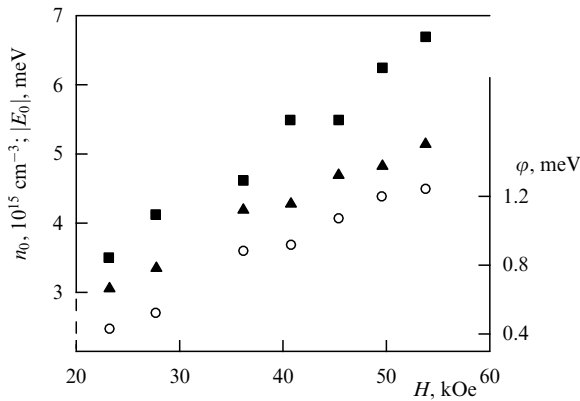


Figure 4. The density (squares) and ground-state energy (triangles) of magnetically stabilized EHL, and the work function of diamagnetic excitons in the liquid (circles) as functions of magnetic field strength.

value being $\Gamma_{av} \cong 0.58$ meV. The dependence of the number density of the magnetically stabilized EHL on magnetic field strength is plotted in Fig. 4. As seen from the figure, magnetically stabilized EHL in indium antimonide compresses considerably with increasing magnetic field strength — in accordance with theoretical expectations [25, 26] and with experimental results for germanium [33].

The work function of excitons in the liquid was determined from the formula

$$\varphi = hv_{ex} - (E_{gL} + E_F), \quad (8)$$

where hv_{ex} is the transition energy to the lowest state of a free diamagnetic exciton. In calculating φ , the values of hv_{ex} obtained from measurements of magnetoreflexion spectra were taken. The values of work function for various magnetic field strengths are given in Fig. 4. These data show that, unlike germanium [33], in indium antimonide the stability of EHL against decay into free excitons grows considerably with increasing magnetic field strength.

In order to determine from experimental data E_0 — the energy per pair of particles in the ground state of a liquid, the quantity whose calculation is central to the theory of EHL — one needs to know the binding energy of diamagnetic excitons because $E_0 = E_{ex} - \varphi$. We utilized the values of E_{ex} (courtesy of A.I. L'Efros) obtained by processing oscillating magnetoab-

sorption spectra [34] based on the theory of Gel'mont et al. [35]. The energy per pair of particles in the ground state of electron – hole liquid is shown as a function of field strength in Fig. 4.

Let us note here two important points revealed by the analysis of the shape of the EHL luminescence band. It turned out, first, that over the entire investigated range of existence of magnetically stabilized EHL, the ultraquantum case occurs only for electrons. Holes populate the two lowest magnetic subbands. In a magnetic field of strength $H = 23$ kOe, only 28% holes bound into EHL occupy the higher-energy subband. As the field strength increases to $H = 55.2$ kOe, their relative number decreases to 12%.

And, second, in order to satisfactorily fit the theoretical spectra to the experimental ones, the temperature in the Fermi distributions f_e and f_h in expression (6) was taken to be lower (by about 10%) than that of the helium bath. It turned out, in other words, that over the entire investigated range of magnetic field strengths the EHL temperature is lower than that of the crystal. At present we do not have a satisfactory explanation for this fact.

The experiments described above made it possible to determine the basic thermodynamic parameters and characteristic energies of a magnetically stabilized EHL in indium antimonide and to see how they behave when the magnetic field strength is varied (see Fig. 4). Let us compare the results obtained with what the theory of strongly compressed EHL in an ultrahigh magnetic field predicts [25, 26]. It should be stressed at once that this theory does not apply to our case directly because strong compression conditions [i.e., ones imposed by the left half of inequality (3)] are not fulfilled for the actual densities of the liquid phase (see Fig. 4). Besides, as already noted, the ultraquantum limit for holes has not yet been achieved in the magnetic field range investigated. At a qualitative level, however, a comparison with the theory does make sense.

For the equilibrium EHL number density, the theory gives

$$n_0(H) \cong 0.03 \left(\frac{m_h}{m_e} \right)^{1/7} \left(\frac{a_{ex}}{a_H} \right)^{16/7} a_{ex}^{-3} \propto H^{8/7}, \quad (9)$$

and for the energy per pair of particles in the ground states of the liquid we have

$$E_0(H) \cong -0.84 E_{ex} \left(\frac{m_h}{m_e} \right)^{2/7} \left(\frac{a_{ex}}{a_H} \right)^{4/7} \propto H^{2/7}. \quad (10)$$

The results presented in Fig. 4 show that as the field strength increases, the liquid density grows somewhat more slowly than predicted by expression (9), and the energy per pair of particles grows much faster than suggested by formula (10). Note that the theory of highly compressed EHL consisting of electrons and holes with greatly differing masses gives (in the case where the ultraquantum situation occurs only for the lighter carriers) an E_0 vs. H dependence (specifically, $E_0 \propto H^{2/5}$) which is stronger than that following from Eqn (10); however, in this case n_0 also increases faster with increasing field strength ($n_0 \propto H^{6/5}$) [36].

The density and energy per pair of particles in the ground state of EHL estimated, respectively, from formulas (9) and (10) for $m_e = 0.014m$, $m_h = 0.075m$, $a_{ex} = 800$ Å, and $|E_{ex}| = 0.5$ meV are compiled in Table 2 for two field strengths, $H = 23$ kOe and 55.2 kOe together with experimental values of these quantities. The calculated liquid

Table 2. Ground-state density and energy, as well as parameters r_s^H and r_s of magnetically stabilized EHL for $H = 23.0$ and 55.2 kOe.

H , kOe	Theory		Experiment			
	$ E_0 $, meV	n_0 , 10^{15} cm^{-3}	$ E_0 $, meV	n_0 , 10^{15} cm^{-3}	r_s^H	r_s
23	1.7	2.6	3.0	3.2	1.5	0.56
55.2	2.1	7.0	5.2	6.7	1.6	0.41

densities agree surprisingly well (apparently fortuitously) with experimental data, whereas the ground-state energies are greatly underestimated as compared with experiments. However, in light of what was said above about the applicability of the theory in question to our results, one can hardly expect any quantitative agreement with experimental data. Note that for EHL in an indium antimonide, the conditions of validity of this theory are fulfilled well in magnetic fields with $H > 1$ MOe.

The theory of EHL in a strong magnetic field predicts the appearance of a dielectric gap in its spectrum due to the one-dimensional motion of charge carriers [25, 37], with dielectric liquid most probably forming at the ‘intermediate’ values of the magnetic field strength [37]. Our observation of EHL ‘overcooling’ relative to the crystal lattice possibly suggests that the EHL electron spectrum ‘becomes dielectric’.

In conclusion, let us compare the density of magnetically stabilized EHL in InSb with that of EHL for $H = 0$ in other materials. As is customary, we will characterize the density by a dimensionless parameter r_s , to which we append a superscript H to emphasize that in our case r_s involves the exciton volume at a given field strength, i.e., $r_s^H = [(4/3)\pi a_{\text{ex}}^2 a_H^2 n_0]^{-1/3}$. As the field strength was increased from 23 to 55.2 kOe, the parameter r_s^H changed from 1.5 to 1.6, which is within experimental error. These values of r_s^H are larger than for EHL in Ge ($r_s = 0.5$) and Si ($r_s = 0.86$) but smaller than in direct band semiconductors ($r_s \approx 2$) and approximately correspond to r_s values in highly deformed Ge and Si [20–22]. If, however, r_s is calculated using the exciton volume in the absence of a field, i.e., $r_s = [(4/3)\pi a_{\text{ex}}^3 n_0]^{-1/3}$, it is found (see Table 2) that, in strong magnetic fields, magnetically stabilized EHL in indium antimonide has a record relative density.

4. Conclusions

The study of indium antimonide shows that EHL stabilized by a strong magnetic field and magnetically stabilized EICs can be created in semiconductors. Magnetically stabilized EICs can form on those impurities unable to bind an exciton in the absence of a magnetic field. The discovered EICs constitute the diamagnetic exciton bound on a neutral shallow acceptor. In the pure n-InSb samples investigated, up to three various EICs corresponding to shallow acceptors of a certain chemical nature were observed.

In indium antimonide, EHL is stable in magnetic fields of strength $H > 20$ kOe. Unlike EHL in unstrained germanium, which was studied in a magnetic field of strength up to 190 kOe [33], in indium antimonide increasing magnetic field strength leads to an increase not only in the density and the energy per pair of particles in the ground state of the liquid but also in the work function of excitons in the electron – hole liquid — that is, enhances the stability of the liquid.

Magnetically stabilized EHL with properties similar to those of EHL in indium antimonide has also been discovered in highly deformed germanium [38].

In our view, it would be very interesting if experiments similar to those described in this paper were performed in stronger magnetic fields. In that case it would be possible to study the basic thermodynamic parameters of EHL as functions of the magnetic field strength in situations in which the ultraquantum limit is achieved not only for electrons but also for holes; to examine the possibility of dielectric liquid to form; to see whether the metal – insulator transition can occur in the liquid phase, and to study many other interesting phenomena [25, 36, 37].

It should be stressed that the study of EHL and other electron systems in a strong magnetic field is not only of interest in itself, because the results obtained can also be applied to systems which have a quasi-one-dimensional electronic spectrum in the absence of a magnetic field [26]. Note that experimental research into conditions for the existence of EHL in quasi-one-dimensional and other reduced-dimensionality systems is, actually, still in its infancy and can be of great interest for the study of interparticle interactions in such systems.

Acknowledgments. I express my sincere gratitude to I V Kavetskaya, V A Tsvetkov, and N V Zamkovets for their cooperation in performing the work presented here; to L V Keldysh for his interest and many fruitful discussions of the points considered in this paper; to Al L Efros for the discussion of our results and for providing calculated data on exciton binding energies and valence band structure in indium antimonide, and to M L Skorikov for discussions and friendly help.

References

1. Yafet Y, Keyes R W, Adams E N *J. Phys. Chem. Solids* **1** 137 (1956)
2. Larsen D M *J. Phys. Chem. Solids* **29** 271 (1968)
3. Raymond A et al. *J. Phys. C: Solid State Phys.* **17** 2381 (1984)
4. Elliott R J, Loudon R *J. Phys. Chem. Solids* **8** 382 (1959)
5. Elliott R J, Loudon R *J. Phys. Chem. Solids* **15** 196 (1960)
6. Gor'kov L P, Dzyaloshinskii I E *Zh. Eksp. Teor. Fiz.* **53** 717 (1967) [*Sov. Phys. JETP* **26** 449 (1968)]
7. Zakharchenya B P, Seisyan R P *Usp. Fiz. Nauk* **97** 193 (1969) [*Sov. Phys. Usp.* **12** 70 (1970)]
8. Sladek R J *J. Phys. Chem. Solids* **5** 157 (1958)
9. Seisyan R P *Spektroskopiya Diamagnitnykh Eksitonov* (Spectroscopy of Diamagnetic Excitons) (Moscow: Nauka, 1984)
10. Kharchenko V A *Zh. Eksp. Teor. Fiz.* **83** 1971 (1982) [*Sov. Phys. JETP* **56** 1140 (1982)]
11. Dujardin F, Stebe B, Munschy G *Phys. Status Solidi B* **141** 559 (1987)
12. Rashba E I, Gurgenshvili G *E Fiz. Tverd. Tela* **4** 1029 (1962)
13. Rashba E I *Fiz. Tekh. Poluprovodn.* **8** 1241 (1974)
14. Rashba E I, Sturge M D (Eds) *Excitons* (Modern Problems in Condensed Matter Sciences, Vol. 2) (Amsterdam: North-Holland, 1982) [Translated into Russian (Moscow: Nauka, 1985)]
15. Kavetskaya I V et al. *Pis'ma Zh. Eksp. Teor. Fiz.* **36** 254 (1982) [*JETP Lett.* **36** 311 (1982)]
16. Kavetskaya I V, Sibel'din N N *Pis'ma Zh. Eksp. Teor. Fiz.* **38** 67 (1983) [*JETP Lett.* **38** 76 (1983)]
17. Kulakovskii V D, Kukushkin I V, Timofeev V B *Zh. Eksp. Teor. Fiz.* **81** 684 (1981) [*Sov. Phys. JETP* **54** 366 (1981)]
18. Gadiyak G V, Lozovik Yu E, Obrekht M S *Fiz. Tverd. Tela* **25** 1063 (1983)
19. Korolev A V, Liberman M A *Phys. Rev. A* **45** 1762 (1992)
20. Rice T M, in *Solid State Physics* Vol. 32 (Eds H Ehrenreich, F Seitz, D Turnbull) (New York: Academic Press, 1977) p. 1 [Translated into Russian (Moscow: Mir, 1980) p. 11]

21. Hensel J C, Phillips T G, Thomas G A, in *Solid State Physics* Vol. 32 (Eds H Ehrenreich, F Seitz, D Turnbull) (New York: Academic Press, 1977) p. 88 [Translated into Russian (Moscow: Mir, 1980) p. 101]
22. Jeffries C D, Keldysh L V (Eds) *Electron-Hole Droplets in Semiconductors* (Modern Problems in Condensed Matter Sciences, Vol. 6) (Amsterdam: North-Holland, 1983) [Translated into Russian (Moscow: Nauka, 1988)]
23. Tikhodeev S G *Usp. Fiz. Nauk* **145** 3 (1985) [*Sov. Phys. Usp.* **28** 1 (1985)]
24. Keldysh L V, Sibeldin N N, in *Nonequilibrium Phonons in Nonmetallic Crystals* (Modern Problems in Condensed Matter Sciences, Vol. 16, Eds W Eisenmenger, A A Kaplyanskii) (Amsterdam: North-Holland, 1986) p. 455
25. Keldysh L V, Onishchenko T A *Pis'ma Zh. Eksp. Teor. Fiz.* **24** 70 (1976) [*JETP Lett.* **24** 59 (1976)]
26. Andryushin E A et al. *Pis'ma Zh. Eksp. Teor. Fiz.* **24** 210 (1976) [*JETP Lett.* **24** 185 (1976)]
27. Kavetskaya I V, Sibel'din N N, Tsvetkov V A *Zh. Eksp. Teor. Fiz.* **105** 1714 (1994) [*JETP* **78** 926 (1994)]
- doi> 28. Kavetskaya I V, Sibeldin N N, Tsvetkov V A *Solid State Commun.* **97** 157 (1996)
- doi> 29. Kavetskaya I V et al. *Zh. Eksp. Teor. Fiz.* **111** 737 (1997) [*JETP* **84** 406 (1997)]
30. Kanskaya L M, Kokhanovskii S I, Seisyan R P *Fiz. Tekh. Poluprovodn.* **13** 2424 (1979)
31. Kavetskaya I V et al. *Zh. Eksp. Teor. Fiz.* **100** 2053 (1991) [*Sov. Phys. JETP* **73** 1139 (1991)]
32. Kavetskaya I V, Sibel'din N N, Tsvetkov V A *Fiz. Tverd. Tela* **34** 857 (1992) [*Sov. Phys. Solid State* **34** 458 (1992)]
- doi> 33. Störmer H L, Martin R W *Phys. Rev. B* **20** 4213 (1979)
34. Kokhanovskii S I, Thesis for Candidate of Physico-Mathematical Sciences (Leningrad: Ioffe Physico-Technical Institute, 1982)
35. Gel'mont B L et al. *Fiz. Tekh. Poluprovodn.* **11** 238 (1977)
36. Keldysh L V *Contemp. Phys.* **27** 395 (1986)
37. Silin A P, in *Electron-Hole Droplets in Semiconductors* (Modern Problems in Condensed Matter Sciences, Vol. 6, Eds C D Jeffries, L V Keldysh) (Amsterdam: North-Holland, 1983) p. 619; [Translated into Russian (Moscow: Nauka, 1988) p. 449]
- doi> 38. Chernenko A V, Timofeev V B *Zh. Eksp. Teor. Fiz.* **112** 1091 (1997) [*JETP* **85** 593 (1997)]

PACS numbers: **41.20.-q**, **78.67.-n**

DOI: 10.1070/PU2003v046n09ABEH001657

Spontaneous atomic radiation in the presence of nanobodies

V V Klimov

1. Introduction

Due to the rapid development of nanotechnologies, it is important to know how nanobodies, i.e., bodies that are small compared to the emission wavelength, influence various optical phenomena. The corresponding subject is called *nanooptics* and plays a special role in optics, since optical effects in the vicinity of nanobodies are determined by the typical sizes of the nanobodies rather than the emission wavelength. At smaller spatial scales, the concentration of electromagnetic fields near the objects increases. Therefore, nanobodies can be efficiently used in nanotechnologies, in developing scanning microscopes with nanometer resolution, in nonlinear optical elements, and in other applications like control of fluorescence and spontaneous emission.

Enhancement or inhibition in the rate of spontaneous emission for an atom in a cavity, which was predicted in Refs [1, 2], was observed in a series of experimental works [3–10]

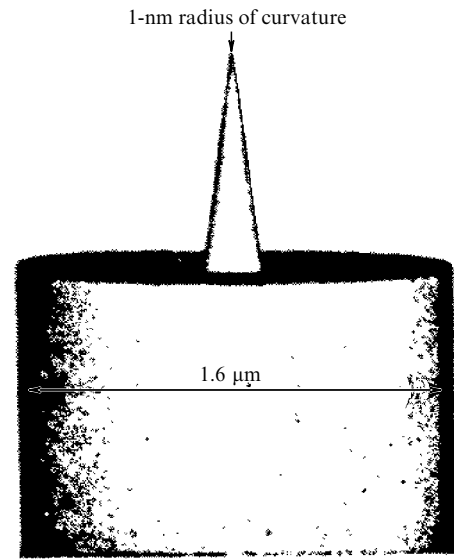


Figure 1. Photograph of a scanning microscope tip made by means of a tunnel electron microscope. The radius of tip curvature is about 1 nm [11, pp. 131–139].

where the cavity size was essentially larger than or comparable to the emission wavelength.

In practice, however, it is often important to find out how nanobodies influence the spontaneous emission of an atom. Such problems arise first of all in the studies of isolated molecules by means of aperture and aperture-free scanning microscopes. Figure 1 shows a typical nanobody, namely the tip of an aperture-free scanning microscope [11]. Nanoparticles of various shapes are also used for controlling fluorescence [12]. In practice, it is sometimes important to elucidate the influence of nanofibres or nanowires on the spontaneous emission of atoms [13–16].

In the present work, we study the effect of nanobodies of various shapes (spherical, spheroidal, cylindrical, etc.) and a round nano-aperture on the spontaneous emission of an atom placed in their vicinity. Our aim is to find the conditions under which spontaneous emission of atomic particles can be efficiently controlled.

2. Theory of the spontaneous emission of atoms in the presence of nanobodies

If the interaction between the atom and the nanobody is weak, i.e., in the case of exponential radiative decay, the expression for the line width γ has the form [17, 18]

$$\frac{\gamma}{\gamma_0} = 1 + \frac{3}{2} \operatorname{Im} \frac{\mathbf{d}_0 \mathbf{E}^R(\mathbf{r}, \mathbf{r}, \omega_0)}{d_0^2 k^3}, \quad (1)$$

where $\mathbf{E}^R(\mathbf{r}, \mathbf{r}, \omega_0)$ describes the reflected field of the dipole \mathbf{d}_0 in the vicinity of the nanobody at the frequency ω_0 of the atom emission and at point \mathbf{r} where the atom is placed. It can be found by solving the Maxwell equations. Other parameters in Eqn (1) are as follows: γ_0 , the line width in vacuum, and $k = \omega_0/c$.

Expression (1) governs the total decay rate of an atom, i.e., the rate at which the radiated energy goes to infinity and is absorbed by the nanobody. It is valid for bodies made of any material. It is worth noting that relation (1) can be used for solving both classical and quantum-mechanical problems